International Journal of Advanced Trends in Engineering and Management
(ISSN 2583-7052)

Vol. IV, No. 10, pp. 1-12, October

Deep Learning Driven Intelligent Colon Cancer Classification Using Attention-Driven Residual Transformer Network

M. Bhuvaneswari[1], M. Swapnaa[2], S. Elakkia Kani[3], V. Sathya[4]

[1]Assistant Professor, Department of Information Technology, R.V.S. College of Engineering, Dindigul.
sakthi.bhuvana4@gmail.com

[2]Assistant Professor, Department of Information Technology, R.V.S. College of Engineering, Dindigul.
manoswapnaa@gmail.com

[3]Assistant Professor, Department of Information Technology, R.V.S. College of Engineering, Dindigul.
elakkia.k91@gmail.com

[4]Assistant Professor, Department of Information Technology, R.V.S. College of Engineering, Dindigul.
sathyav265@gmail.com

[1*]**Corresponding Author E-mail:** sakthi.bhuvana4@gmail.com

ABSTRACT: Early detection of colorectal cancer in medical imaging is important for improving patient outcomes and guiding treatment strategies. In order to classify the colon cancer, this study proposes the automated image analysis system that integrates deep learning driven classification. The Adaptive Non-Local Means (ANLM) filter is initially employed to denoise the colon cancer images while preserving fine structural and textural characteristics. To enhance border consistency and region homogeneity, spatially constrained K-means clustering is used to accurately segment the malignant areas by leveraging spatial neighborhood information. From the segmented areas, Gray Level Co-occurrence Matrix (GLCM) is applied to extract the discriminative textural features, capturing vital statistical information regarding tissue heterogeneity and morphological changes. The dataset named Lung and Colon Cancer Histopathological Images dataset is used which is available in kaggle. An Attention-Guided Residual Transformer Network (AGRT-Net), which blends residual learning with self-attention processes to model long-range dependencies and highlight diagnostically relevant aspects, is then used to classify these features. By focusing on cancer patterns, the proposed model improves the feature discrimination. Using the Python software, the AGRT-Net achieves higher uniform value of 0.979 across the accuracy, precision, recall, and F1-Score, which demonstrates robust potential for computer-aided colon cancer diagnosis.

Keywords: Colon cancer classification, histopathological image analysis, spatially constrained K-means clustering, Gray Level Co-occurrence Matrix (GLCM), and Python.

1. Introduction

Colorectal cancer (CRC) is the leading cause of cancer incidence and mortality on global scale. Early detection and accurate classification of CRC is hypercritical for improving patient results and directing therapeutic strategies. Conventional diagnostic methods rely heavily on manual histopathological analysis, which is labor-intensive and prone to inconsistent interpretations, highlighting the requirement for more effective diagnostic tools [1]. According to WHO classification, the main histological types of CRC involves papillary, mucinous, and signet-ring cell variants, along with less common forms like squamous cell, carcinoid carcinomas, and

adenosquamous. Adenocarcinoma is the most prevalent form of colorectal cancer, accounting for over 90% of cases [2]. This trend highlights that early screening and increasing the awareness are important for enhancing the patient outcomes [3]. The colon cancer treatment, the manual Histopathology Image Analysis (HIA) takes a significant amount of time and assessment of classifying the tissue which is influenced several subjective parameters. Subsequently, the more automated method which is based on the computer-aided diagnosis (CAD) is recently favoured on their consistency [4].

Image pre-processing is the crucial step for the accurate classification of disease images. To enhance the accurate diagnosis in the medical field, denoising and image quality is important. Median filter are the non-linear digital filtering techniques which is used in image processing effectively remove the noise from the image. Although, it is the non-linear filter that replaced the pixel value with middle value of its neighbors after sorting them numerically [5]. The Non-Local Means (NLM) filter provides denoising by averaging pixel values with similar nearest patterns of entire image, which leverages the image redundancy, but it have certain disadvantages, primarily centered on its computation intensity and performance at high noise levels [6]. Normalization converts the pixel intensities from the 0-255 integer range into a 0 to 1 decimal range. Nevertheless, the image normalization reduces the image clarity and erase the important information [7]. The ANLM filter is proposed to removing the noise from the colon cancer images, addressing the limitation from the existing image pre-processing technique, which specifically preserving the delicate textures and edges essential for identifying the cancerous tissue. To segment the relevant cancerous regions, the subsequent image segmentation process is necessary to segment the relevant cancerous areas accurately.

The image segmentation is the process of segments the images into non-overlapping groups. Otsu's technique is the important image segmentation based on the image thresholding and this method shows effective for only when the image histogram has bimodal distribution, this model underperforms in noisy image, low contrast, non-uniform image, especially when predicting small objects or when classes overlap significantly [8]. Fuzzy C-Means offers robust accuracy in image segmentation with overlapping boundaries or low contrast by utilizing membership grades, but it suffers from high computational complexity and poor noise resistance [9]. To overcome these limitation, this study proposed the K-means Clustering for high efficiency, enhancing the border consistency and homogeneity by combining local neighborhood information to separate malignant regions.

To extract the specific image patterns and spatial relationship to classify the colon cancer, the feature extraction is needed. The Dyadic Wavelet Packet Transform (DYWPT) method offers the multi-level frequency analysis for detailed texture decomposition through recursive filtering, but it involves iterative high-pass and low-pass filtering, increases the computational complexity [10]. Local Binary Pattern (LBP) is the robust, lighting invariant approach for face recognition, yet it sensitive in image noise and fails to capture global texture patterns [11]. To addresses these limitation, this work proposes the GLCM based feature extraction which captures the statistical information regarding the spatial relationship and dependencies between pixel intensities which allows extract the high discriminative features that detect any changes in cancerous colon tissue. The accurate colon cancer classification is significant for enabling early, precise diagnosis which slows disease progression and enhance lifetime. The few techniques are reviewed in following section

2. Related Works

Sobur et al., (2024) [12] have developed the hybrid deep learning method with the dual-CNN

structure to classify the colon cancer. This method utilizes the Global Average Pooling (GAP) and dropout regularization, with feature reduction technique to improve efficiency and prevent overfitting. However, the dual-CNN method demands intense computational power for training, despite its performance benefits.

Tiwari et al., (2022) [13] have presented a clinically relevant grade prediction model for colon cancer by using Fourier Transform Infrared spectroscopic (FT-IR) imaging to capture modular data from unlabelled tissue. By using a DL classifier, trained an infrared absorption and morphometric data from 148 patient corhort. However, it is limited by increased complexity and FT-IR equipment cost compare to traditional techniques.

Vanitha et al., (2024) [14] have proposed the hybrid DL framework which integrates the Xception and mobileNet architecture to enhance classification of lung and colon cancer. Proposed method was trained on histopathological images, and use a Grad-CAM for interpretablility. Nevertheless, the proposed model often suffer from overfitting due to imbalanced histopathological datasets.

Kavitha et al., (2022) [15] have proposed the CNN model for automated polyp identification and predicting the colorectal cancer, for enhancing diagnostic accuracy and to optimizing clinical workflows. It examine CNN and transfer learning using image patches from endoscopic and histological images. Nonetheless, the proposed method lack transparency, reliability and undermining clinical trust and diagnostic equity.

Sharkas et al., (2024) [16] have developed the Computer-aided diagnostic system for classifying the CRC by using DenseNet201. This employs feature extraction, then Discrete Cosine Transformer (DCT) for dimensionality reduction and spectral representation. Nevertheless, this study provides poor generalizability from static dataset and loses important data during dimensionality reduction.

Mengash et al., (2023) [17] have developed the Deep Belief Networks for classifying the colon cancer by using histopathological image. This research employs the MobileNet for feature vector generation and develop the colon cancer classification. However, the method lacks in computational complexity, does not perform well on new data, and losses the prevalent information during data pre-processing.

Divyashree et al., (2025) [18] have presented an advanced Vision Transformer (ViT) architecture to enhance the accurate colorectal cancer classification in clinical setting. By using patch based ViT and self-attention mechanism, it extracts the subtle morphological features from histopathology image to improve the diagnostic accuracy. Although, this study lacks in interpreting complex global features representation for clinics.

Ke et al., (2025) [19] have developed convolutional neural networks model for CRC diagnosis using TL and multi-model feature fusion to address image complexity. The framework provides multi head self-attention and MLP classifier which evaluated across several dataset. However, it lacks in potential interpretability problems inherent in complex fusion models.

1.1 Objectives

- To implement high-fidelity denoising using an ANLM filter to remove noise while preserving essential structural and textural details in colon cancer images.
- To achieve precise tumor segmentation by applying spatially constrained K-Means clustering to accurately isolate malignant regions while maintaining border consistency.
- To extract discriminative texture features utilizing the GLCM to capture statistical

tissue characteristics and morphological changes vital for diagnosis.

- To develop an advanced classification architecture using an AGRT-Net to model long-range dependencies and highlight prominent cancerous patterns.

3. Proposed System

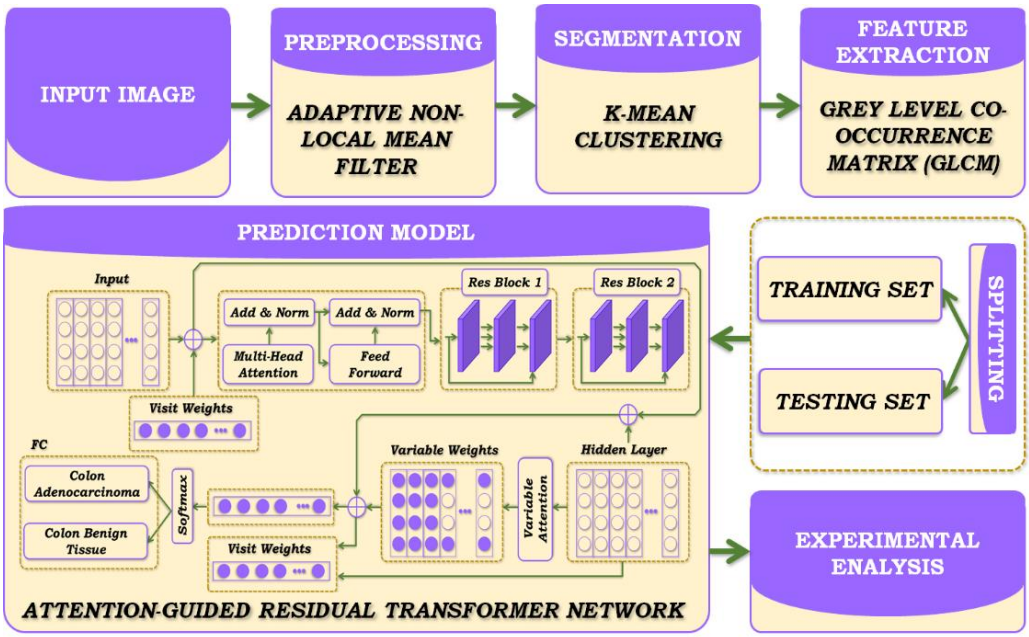

Figure 1: *Block diagram for the proposed model*

Figure 1 depicts the suggested model, automated system to classifying the colon cancer. The first stage is pre-processing stage which undergo ANLM Filter for noise reduction, followed by spatially constrained K-means clustering is utilized for segmenting the malignant regions while maintaining border consistency. Then the GLCM is used to extract the features for to capture statistical tissue characteristics and morphological changes. The extracted features are serves as an input to the AGRT-Net model to generate the colon cancer classification. In the final stage, this study analyse the performance of AGRT-Net model which generates the result to determine the precise classification of colon cancer.

4. Proposed Sytem Modelling

4.1 Data Preprocessing By Adaptive Non-Local Means Filter

ANLM filter improve the colon histopathology images by leveraging redundant local structures to decrease the noise through weighted average pixel intensity. The weights are mathematically calculated as in eqn. (1)

$$w(x,y) = exp\left(-\frac{\sum_{\delta \epsilon P} G_\sigma(\delta)[u(x+\delta)]-u(j+\delta)^2}{h^2}\right) \quad (1)$$

where, G_σ denotes as Gaussian kernel, P indicates the patch centered at the position x, y and the weight is determined by measuring the distance between two pixel patches and the smaller square brightness difference result in higher weights. h is the smoothing parameter, which provides the specific noise level of cancerous tissue, and preserves the important morphological details and textural characteristics.

This filter addresses the limitation like high computational cost of standard through integral images for sum-squared difference calculation, lookup table for exponential functions and GPU acceleration, which results increasing speed effectively. The ANLM filter removes the noise in medical imaging by adjusting parameter locally based on noise map, and preserves the fine

structural and textural characteristics which distinguish the colon adenocarcinoma and benign colon tissue.

4.2 Spatially Constrained K- Means Clustering

The pre-processing data is inputted into the using K-Means clustering to accurately isolate the malignant regions while maintaining border consistency. The algorithm divides the dataset into K clusters by utilizing distance metrics to establish initial centroids, then define the individual cluster by the mean value of its assigned data points. This iterative process partitions the image data points$\{x_1, x_2, \dots \dots . x_k\}$ into disjoint sets $\{N_1, N_2, \dots \dots . N_k\}$ to separate the tumor region by minimal average squared distance individual point and its assigned as cluster centroid. It is mathematically represented as in eqn. (2)

$$\underset{N^n}{argmin}\frac{1}{n}\sum_{i=1}^{k}\sum_{x\in N_i}||x-\delta_i||^2 \qquad (2)$$

Where, δ_i denotes as mean of points in N_i.

Assign each point to the cluster with the similar centroid nearer to the point, which is calculated in eqn. (3)

$$N_i^{(t)} = \{x: \| x-\delta_i{}^{(t)} \|^2 \leq \| x-\delta_i{}^{(t)} \|^2 \ \forall j, 1 \leq j \leq k\} \qquad (3)$$

The cluster centers is updated by computing the average position of all data points within the category and mathematically represented in eqn. (4)

$$\delta_i{}^{(t+1)} = \frac{1}{|N_i{}^{(t)}|}\sum_{x_j\in N_i} x_j \qquad (4)$$

Verify the centroid (δ) and the objective function, total within cluster sum of squares have stabilized. The condition $\delta^{(t+1)} = \delta^t \forall i \leq k$ implies that the algorithm is converges, which means the cluster assignment and centroid no longer changes between the iteration, when if the maximum iteration limit is reached. The outcome of this segmentation is refined binary segmented mask that describe colon region from benign tissue, offering localized region of interest, homogeneous regions and structural fidelity for subsequent analysis.

4.3 Grey Level Co-Occurance Matrix

After the segmentation, GLCM is used for extracting features in histopathological images to capture spatial and greyscale distribution, especially efficient for analyzing stochastic textures. This technique involves computing the frequency of pixel brightness pairing across several distance and angle. The first order texture measurements employs statistical calculation depends on each pixel intensity, does not concern the spatial dependencies or relations between neighbouring pixels. Secondly, the inter-relationship of the initial pixel pairs is taken into the process. GLCM is mathematically expressed in eqn. (5)

$$GLCM_{\vec{r}}(i,j) = \left|X\left(l_i, m_j\right), X\left(l_i, m_j\right)\right|\vec{r} = \sqrt{\left(l_i - l_j\right)^2 + \left(m_j - m_i\right)^2}, \quad i,j \in N \quad where\ 0 \leq X(l,m) \leq 225 \qquad (5)$$

There are four key statistical features which is consist of energy, contrast, correlation, and homogeneity which is extracts from the GLCM to offer high level information about tissue characteristics and morphological changes, aiding in diagnostic system soundness by highlighting the relevant component. The result provides a refined set of high-level textural signature quantifying tissue heterogeneity and morphological changes, which serves as input for the ACRT-Net classification stage.

4.4 Attention-Guided Residual Transformer Network (Agrt-Net)

The texture enhance data is then passed to ResNet-18 for deep feature extraction. ResNet-18 is combined as the main feature extraction backbone to leverage its strong residual learning abilities. The architecture used the residual blocks to address the degradation issue typically gathered in deep network, enabling for the capture of complex morphological patterns in tissue. The fundamental

operation of these blocks is expressed mathematically in eqn. (6)

$$x = H(y, \{F_i\}) + y \quad (6)$$

Here, x represents the input block, $H(y, \{F_i\})$ denotes the residual mapping to learn across the conventional weights F_i and x indicates the final output. By comprising these identify shortcut connection, the method confirm the smooth gradient propagation, mitigating the risks of vanishing gradients effectively. Among the ResNet family, the ResNet 18 model is particularly selected for this study to balancing the high diagnostic performance with computational efficiency. It contains 18 layers which offers the streamlined structure that necessary for fewer storage and memory resources compares to deeper architecture such as ResNet-50 or RestNet 101. This effectiveness allows quick training and inference cycles, which makes it most suitable for real time clinical decision support system which maintains the deep necessary to extract discriminative histopathological features from complex colon cancer image.

The model combines a hybrid embedding strategy where the ResNet-18 backbone extracts the spatial features. The feature maps are the passed into the series of continuous vector for processing by the transformer layers. The mathematical expression of resulting inputs sequence L_i is defined as in eqn. (7)

$$L_i = E(y_i) + P_i \quad (7)$$

Here, $E(y_i)$ is the deep spatial embedding and P_i represents the positional encoding. This approach prevents the local textural representation from the ResNet-18 model, global positional context for the self-attention mechanism. The transformer encoder layer process the feature embedded sequence to map intricate relationship in the colon cancer tissue data. Every layer utilizes the Multi head Self Attention to extract high dimensional representation, with the final encoded output which is computed as,$E(x) = [e_1(x), e_2(x), \ldots\ldots, e_n(x)]$, where $e(x)$ indicates positional output vector. The transformer model uses the self-attention mechanism to find higher order interactions and non-adjacent feature correlation, which computes the attention weight (a_w) which show the relative importance of position. It is expressed in eqn. (8)

$$a_w = softmax\left(\frac{Q_v^R K_e}{\sqrt{dk}}\right) \quad (8)$$

Where, Q_v and K_e are the query and key corresponding to the input embedding $e_1, e_2, \ldots\ldots, e_n$. The weights are derived from the vectors are utilized to generating output vectors by summing weighted value representation. The model handles the variable sequence lengths by using the padding mask and incorporates embedding layers to capture the feature essence and order information.

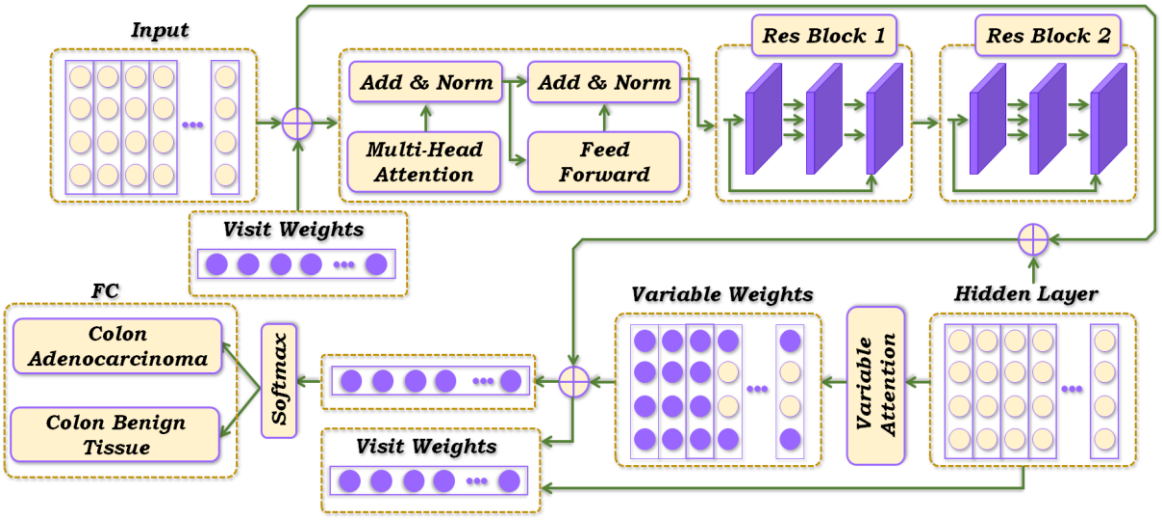

Figure 2: *Proposed model architecture*

The self –attention output is passes through the Feed Forward Network (FFN) comprising of 2 linear transformation which separates by non-linear activation function. To confirm stable gradient flow and deep feature combination, residual connection are used after both self-attention and FFN sub layers. Every phase concludes with layer normalization that stabilizes the hidden state and improves overall convergences efficiency

The output from the transformer decoder stack is fed into fully connected layer. The softmax layer is then applied to determine the final output probabilities, which enables the accurate classification of colon adenocarcinoma and colon benign tissue. It is expressed in eqn. (9)

$$y = softmax(V_a + e) \quad (9)$$

Here, V_a indicates the learned weights parameter and e indicates the final encoded feature vector.

5. Result and Discussion

This section describes the experimental outcome for AGRT-Net model for classifying the colon cancer. The images used in this result section is taken from the Lung and Colon Cancer Histopathological Images dataset. The result is implemented by python software.

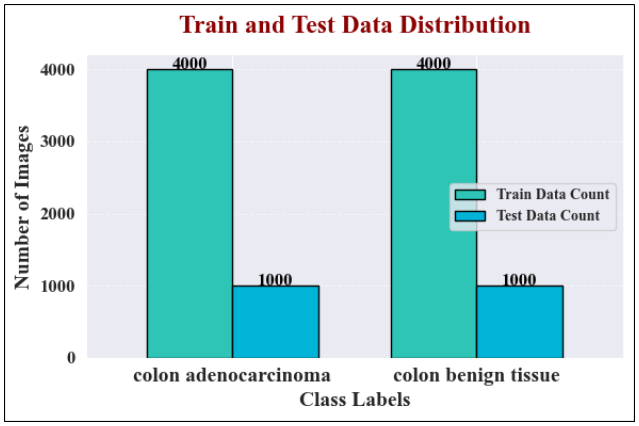

Figure 3*: Data Distribution per class*

The figure 3 illustrates the histopathological image among with testing and training set of the two classes of colon cancer. The training and testing images reveals the 4000 colon adenocarcinoma and 1000 benign colon tissue. This balanced distribution underscores the equal representation of the data and eliminates the prevalence of one of the classes in learning, which enhance the clinical applicability of the model in real-world scenarios.

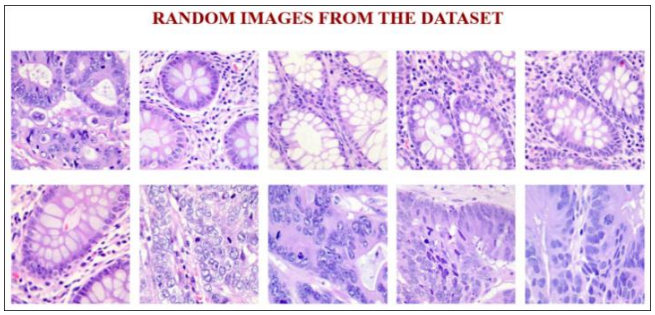

Figure 4: *Sample image from the dataset*

Figure 4 illustrates the 10 sample histopathological images of the colon cancer is taken from dataset. The standard hematoxylin-eosin with specific purple and pink coloring that demonstrate the cellular and morphological characteristics, enabling the observation of changes in glandular structure, tissue organisation.

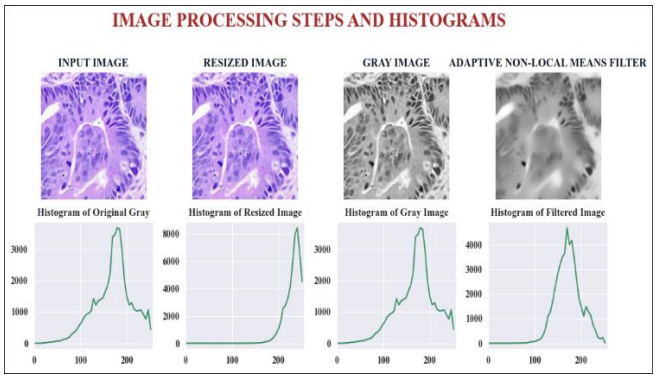

Figure 5: *Image Processing Steps and Histograms*

Figure 5 shows the series pre-processing pipeline used to process histopathological images, and the pixel intensity histograms at every step. The pixel intensity values ranges from 0 to 255 across all the charts. The frequency of these pixel differs, with peak count reaching approximately 3000 in the original and gray images, up to 8000 in the resized image and around 4000 after filtering. This uniform pre-processing which makes the image quality clear and effective feature distillation in the model training process.

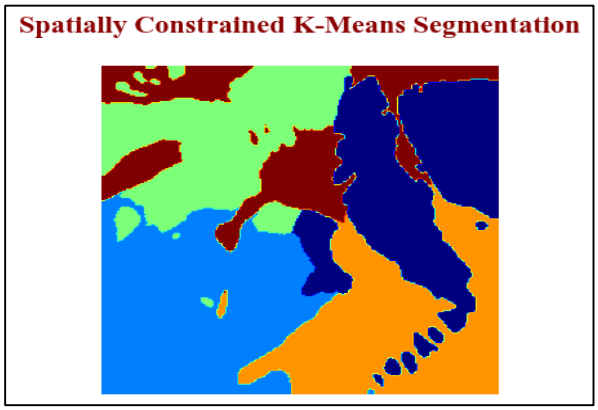

Figure 6: *Spatially Constrained K-Means Segmentation*

This figure 6 shows the output of spatially constrained K-means clustering on a histopathological image, where the various tissue areas are divided with the help of different color codes. The algorithm clusters pixels using similarity in intensity and proximity, which permits useful division of histological constituents. Colored areas indicate glandular lumens, nuclei, cytoplasm and stromal tissue structures. This segmentation makes further analysis easier and better the model to learn discriminative tissue patterns to be able to classify them correctly.

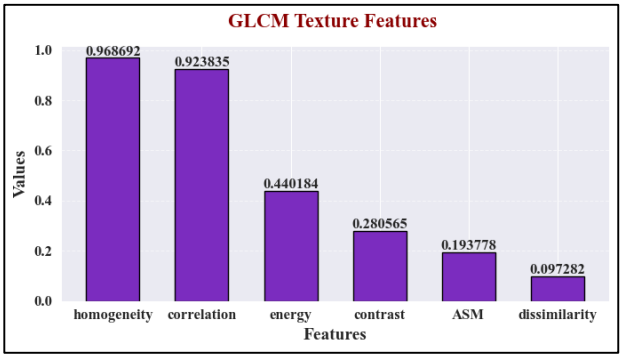

Figure 7: *GLCM texture features*

The figure 7 shows the texture features of histopathological images based on GLCM utilized in the classification of images. Six essential descriptor are illustrates in this image with the homogeneity which provides the high value of 0.9686, uniformity between adjacent pixel intensities, which the dissimilarity shows the lowest value of 0.097 and energy, contrast and ASM shows the intermediate values, providing a quantitative basis for the textural analysis.

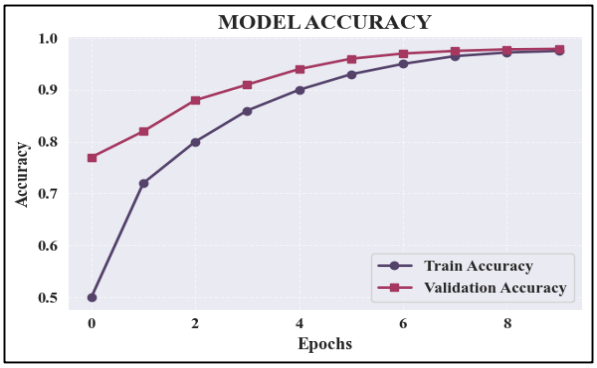

Figure 8: *Model Accuracy*

This figure 8 represents the training accuracy and validation accuracy of AGRT-Net method regarding ten epochs. The training accuracy increases at a high rate starting at approximately 0.50 whereas validation accuracy begins at approximately 0.77 and slowly increases. Both curves have a consistent and smooth upward trend which attains about 0.98 in the last epoch. The low difference between training and validation accuracies suggests that there is high generalization with little overfitting.

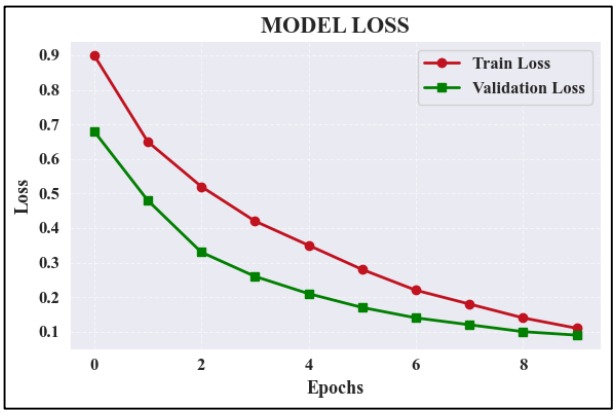

Figure 9: *Model Loss*

Figure 9 shows the training and validation loss of in the learning process of the AGRT-Net method. The training loss reduces gradually between 0.90 and 0.11 showing that there is an efficient minimization of error on the training set and validation loss decreases gradually between approximately 0.68 and 0.09, which is right after the training curve. The two curves are almost parallel indicates high generalization and no

overfitting, which provide accurate classification of colon cancer.

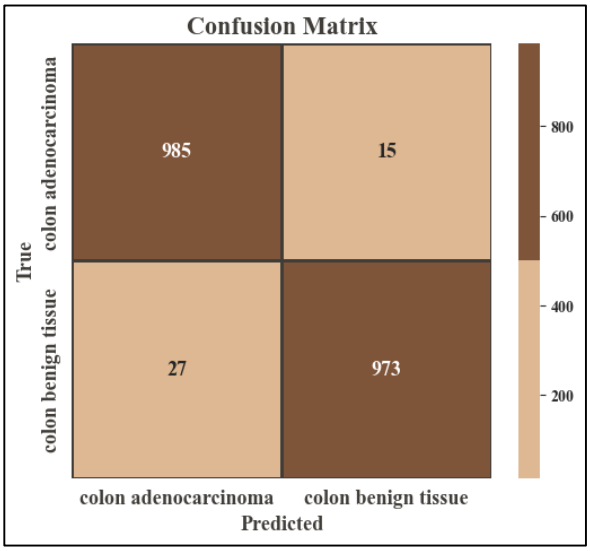

Figure 10: *Confusion matrix*

The figure 10 depicts the confusion matrix which evaluates a model performance in classifying colon cancer. The AGRT-Net model achieves 985 true positive for adenocarcinoma and 973 true negatives for benign tissue, which indicates the robust predictive capabilities. It records only 15 false negative and 27 false positives which indicates highly effective and accurate classification of colon cancer.

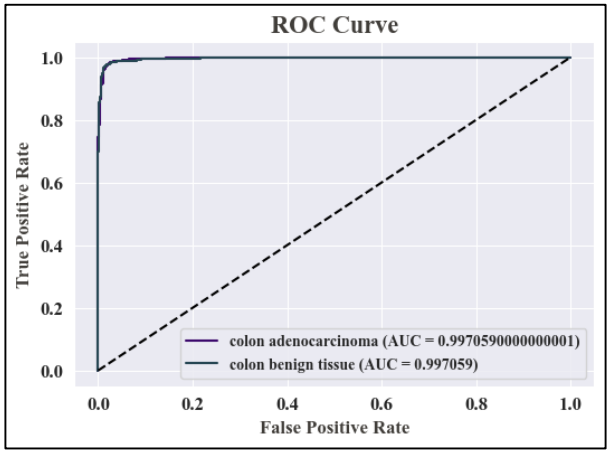

Figure 11: *ROC curve*

Figure 11 displays the ROC curve for a model which classifying the colon tissues model by the plot of the TPR and the FPR at different thresholds. Both classes achieves the high AUC value of 0.997, demonstrating highly reliable separation between colon adenocarcinoma and benign tissues.

5.1 Classification Report

Table 1: *Classification report for the Colon cancer classification*

Class/ metrics	Precision	Recall	F1-Score	Support
Colon adenocarcinoma	0.9773	0.9850	0.9791	1000
Colon benign tissue	0.9848	0.9730	0.9789	1000
Accuracy			0.9790	2000
Macro avg	0.9791	0.9790	0.9790	2000
Weighted avg	0.9791	0.9790	0.9790	2000

Table 1 presents the classification report, detailing the model performance across both colon classes tissues. In the case of colon adenocarcinoma, the model has a high precision of 0.9733, recall of 0.9850 and F1-score of 0.9791 and the benign tissue group shows the good results, the precision of 0.9848, and recall of 0.9730 and F1-score of 0.9789. A total accuracy of 0.9790 on 2000 validation samples is evidence of robust classification.

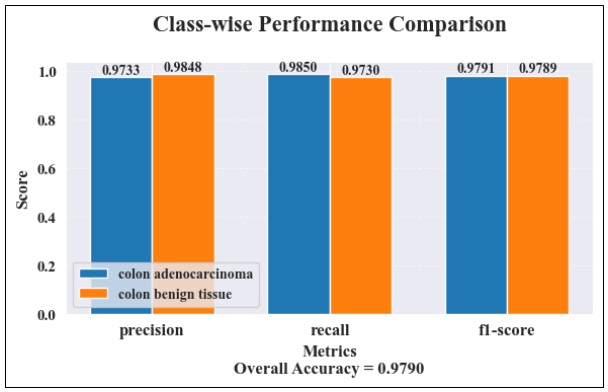

Figure 12: *Class-wise Performance comparison*

Figure 12 shows the comparison of precision, recall, and F1-score of colon adenocarcinoma and

benign tissue classes. The model achieves high accuracy of 97.90% across all metrics. Both classes shows robust result in precision, recall, and F1-score with all values exceeding 0.97. The highest individual metric was a recall of 0.9850 for the adenocarcinoma class, which indicates the robust for classifying the two types tissues.

5.2 Comparative Analysis

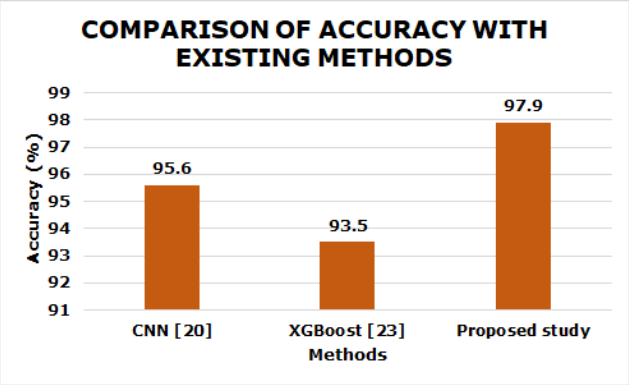

Figure 13: *Comparison of accuracy with existing studies*

Figure 13 depicts the accuracy of an AGRT-Net model with conventional methods for colon cancer classification. AGRT-Net model achieves the superior accuracy of 97.9%. The proposed model have better performance classifying the colon cancer when compared to other method.

Table 2: *Comparison with existing models*

Methods	Precision	Recall	F1-Score
MRANet [21]	0.9440	0.9545	0.9492
AlexNet[22]	0.9672	0.9664	0.9667
Proposed study	0.9791	0.9790	0.9790

The table 2 shows the the comparison of precision and recall of the AGRT-Net model with existing study. The AGRT-Net model achieves the highest precision of 0.979, recall of 0.9790, and 0.9790 of F1-score. When compared with other methods, AGRT-Net model shows the robust value, which indicates the accurate classification of colon cancer.

6. Conclusion

The study proposed the AGRT-Net model to classify the colon cancer. The pre-processing step is significantly reduced the noise and preserved the structural and textural details in colon cancer images by using the ANLM filter. Next, the spatially constrained K-Means clustering is accurately segmented the malignant regions while border consistency. Furthermore, the GLCM used to capture the statistical tissue characteristics and morphological changes for diagnosis. Finally, the proposed model effectively the classified the Colon cancer with superior accuracy. AGRT-Net model achieved high accuracy of 0.979, precision of 0.979, recall of 0.979, and F1-Score of 0.97, which is highly effective compared with existing method. The AGRT-Net is effective method which classified the colon cancer accurately.

Reference

1. Süheyla Demirtaş Alpsalaz; Emrah Aslan; Yıldırım Özüpak; Feyyaz Alpsalaz; Hasan Uzel; Viktoria Bereznychenko, Year: 2025, “Hybrid deep learning with attention fusion for enhanced colon cancer detection”, Scientific Reports.
2. Armaano Ajay; R. Karthik; Akshaj Singh Bisht; Abhay Karan Singh, Year: 2025, “QDeepColonNet: a quantum-based deep learning network for colorectal cancer classification using attention-driven DenseNet and shuffled dynamic local feature extraction network”, Artificial Intelligence Review, Vol: 58, No: 10, pp. 304.
3. Akshaj Singh Bisht; Armaano Ajay; R. Karthik, Year: 2025, “DeepCRC-Net: An Attention-Driven Deep Learning Network for Colorectal Cancer Classification Using Xception and Efficient Lightweight Local Feature Fusion Networks”, IEEE Access.
4. Majdi Khalid; Sugitha Deivasigamani; Sathiya V; Surendran Rajendran, Year: 2024, “An efficient colorectal cancer detection network using atrous convolution with coordinate attention transformer and histopathological images”, Scientific Reports, Vol: 14, No: 1, pp. 19109.

5. Shenbagarajan Anantharajan; Shenbagalakshmi Gunasekaran; Thavasi Subramanian, Year: 2024, “MRI brain tumor detection using deep learning and machine learning approaches”, Measurement: Sensors, Vol: 31, pp. 101026.
6. Tamil Nādu Chidambaram, Year: 2023, “Fractional Stochastic Gradient Descent Trained SM-Segnet-Based Segmentation And Capsule Neural Network For Colon Cancer Detection”, Tuijin Jishu/Journal of Propulsion Technology, Vol: 44, No: 6.
7. Seth R. Shaffer; Amarachi I. Erondu; Cindy Traboulsi; Victoria Rai; Noa Krugliak Cleveland; Amanda Israel; Britt Christensen; David T. Rubin, Year: 2022, “Achieving histologic normalization in ulcerative colitis is associated with a reduced risk of subsequent dysplasia”, Inflammatory Bowel Diseases, Vol: 28, No: 4, pp. 553-559.
8. Osbaldo Vite-Chávez; Jorge Flores-Troncoso; Reynel Olivera-Reyna; Jorge Ulises Munoz-Minjares, Year: 2023, “Improvement procedure for image segmentation of fruits and vegetables based on the Otsu method”, Image Analysis and Stereology, Vol: 42, No: 3, pp. 185-196
9. Necla Koçhan; Barış Emre Dayanç, Year: 2023, “Development of molecular subtype specific prognostic marker signature in immune response associated colon cancer through fuzzy based transcriptomic approach”, medRxiv, pp. 2023-05.
10. Daigo Takano; Hajime Omura; Teruya Minamoto, Year: 2025, “Detection and classification method for early-stage colorectal cancer using dyadic wavelet packet transform”, IEEE Access, Vol: 13, pp. 9276-9289.
11. Shtwai Alsubai, Year: 2024, “Transfer learning based approach for lung and colon cancer detection using local binary pattern features and explainable artificial intelligence (AI) techniques”, PeerJ Computer Science, Vol: 10, pp. e1996.
12. Abdus Sobur; Imran Chowdhury Rana, Year: 2024, “Advancing cancer classification with hybrid deep learning: Image analysis for lung and colon cancer detection”,
13. Saumya Tiwari; Kianoush Falahkheirkhah; Georgina Cheng; Rohit Bhargava, Year: 2022, “Colon cancer grading using infrared spectroscopic imaging-based deep learning”, Applied spectroscopy, Vol: 76, No: 4, pp. 475-484.
14. K. Vanitha; Mahesh T. R; S. Sathea Sree; Suresh Guluwadi, Year: 2024, “Deep learning ensemble approach with explainable AI for lung and colon cancer classification using advanced hyperparameter tuning”, BMC Medical Informatics and Decision Making, Vol: 24, No: 1, pp. 222.
15. Muthu Subash Kavitha; Prakash Gangadaran; Aurelia Jackson; Balu Alagar Venmathi Maran; Takio Kurita; Byeong-Cheol Ahn, Year: 2022, “Deep neural network models for colon cancer screening”, Cancers, Vol: 14, No: 15, pp. 3707.
16. Maha Sharkas; Omneya Attallah, Year: 2024, “Color-CADx: a deep learning approach for colorectal cancer classification through triple convolutional neural networks and discrete cosine transform”, Scientific Reports, Vol: 14, No: 1, pp. 6914.
17. Hanan Abdullah Mengash; Mohammad Alamgeer; Mashael Maashi; Mahmoud Othman; Manar Ahmed Hamza; Sara Saadeldeen Ibrahim; Abu Sarwar Zamani; Ishfaq Yaseen, Year: 2023, “Leveraging marine predators algorithm with deep learning for lung and colon cancer diagnosis”, Cancers, Vol: 15, No: 5, pp. 1591.

18. S. Divyashree; G. Arunsankar; M. Mythily; Lalitha Kalaichelvan; Sasi Vaithilingan; D. Usha; M. Ruba; N. Mohankumar, Year: 2025, “VISION TRANSFORMER ARCHITECTURE FOR ACCURATE COLORECTAL CANCER CLASSIFICATION IN CLINICAL IMAGE ANALYSIS”, INTERNATIONAL JOURNAL OF ADVANCES IN SIGNAL AND IMAGE SCIENCES, Vol: 11, No: 2, pp. 4-57.
19. Qi Ke; Yan Chai Hum; Wun-She Yap; Tian Swee Tan; Humaira Nisar; Hamam Mokayed; AiQuan Li; Rong Gao; YuJian Gan, Year: 2025, “Histopathological classification of colorectal cancer based on domain-specific transfer learning and multi-model feature fusion”, Scientific Reports, Vol: 15, No: 1, pp. 35155.
20. Ahmad Taher Azar; Mohamed Tounsi; Suliman Mohamed Fati; Yasir Javed; Syed Umar Amin; Zafar Iqbal Khan; Shrooq Alsenan; Jothi Ganesan, Year: 2023, “Automated system for colon cancer detection and segmentation based on deep learning techniques”, International Journal of Sociotechnology and Knowledge Development (IJSKD), vol: 15, No: 1, pp. 1-28.
21. Diponkor Bala; SM Rakib Ul Karim; Rownak Ara Rasul; Sraboni Ghosh Joya; Mohammad Alamgir Hossain; Zhaoxian Zhou, Year: 2025, “Mranet: a modified residual attention networks for lung and colon cancer classification”, In 2025 2nd International Conference on Next-Generation Computing, IoT and Machine Learning (NCIM), pp. 1-6. IEEE.
22. Maha Sharkas; Omneya Attallah, Year: 2024, “Color-CADx: a deep learning approach for colorectal cancer classification through triple convolutional neural networks and discrete cosine transform”, Scientific Reports, Vol: 14, No: 1, pp. 6914.
23. Raquel Ochoa-Ornelas; Alberto Gudiño-Ochoa; Julio Alberto García-Rodríguez, Year: 2024, “A hybrid deep learning and machine learning approach with Mobile-EfficientNet and Grey Wolf Optimizer for lung and colon cancer histopathology classification”, Cancers, Vol: 16, no: 22, pp. 3791.